ARTICLE

Preparation and Characterization of Electrodeposited-Annealed $CuInSe_2$ Thin Films for Solar Cells

Zhong-wei Zhang, Hong-yan Guo, Ji Li, Chang-fei Zhu*

CAS Key Laboratory of Materials for Energy Conversion, Department of Materials Science and Engineering, University of Science and Technology of China, Hefei 230026, China

(Dated: Received on November 27, 2010; Accepted on February 12, 2011)

$CuInSe_2$ (CIS) films with good crystalline quality were synthesized by electrodeposition followed by annealing in Se vapor at 530 °C. The morphology, composition, crystal structure, optical and electrical properties of the CIS films were investigated by scanning electron microscopy, energy dispersive spectroscopy, X-ray diffraction, Raman spectroscopy, UV-VIS-NIR spectroscopy, and admittance spectroscopy. The results revealed that the annealed CIS films had chalcopyrite structure and consisted of relatively large grains in the range of 500−1000 nm and single grain of films extend usually through the whole film thickness. The band gap of CIS films was 0.98 eV and carrier concentration was in the order of 10^{16} cm^{-3} after etching the Cu-Se compounds on the film surface. Solar cells with the structure of AZO/i-ZnO/CdS/CIS/Mo/glass were fabricated. Current density *vs.* voltage test under standard reported condition showed the solar cells with an area of 0.2 cm^2 had a conversion efficiency of 0.96%. The underlying physics was also discussed.

Key words: $CuInSe_2$ film, Electrodeposition, Annealing, Solar cell

I. INTRODUCTION

$CuInSe_2$ (CIS) and its based compound films are promising for photovoltaic applications due to their large absorption coefficient, the ability to undergo band engineering by alloy formation and their long-term opto-electronic stability [1−3]. A great deal of efforts have been made to develop low-cost techniques for preparation of CIS thin films [4−9]. The physical deposition processes have shortcomings in terms of the requirements of high vacuum conditions, high production costs and the high toxicity from the precursor H_2Se. An attractive alternative is the low-cost two step electrodeposition-annealing process involving Se vapor to replace the hazardous H_2Se [10, 11]. Electrodeposition is a potentially suitable method to produce CIS films owing to the attractive low cost, low operating temperature, high materials utilization and it can deposit uniform large area materials and can easy adjust the composition by changing chemical or electrical parameters [12−15]. In spite of the large amount of studies on electrodeposited CIS thin films, only a few publications reported solar cell results [16]. The use of electrodeposition to prepare precursor absorber layers has resulted in $Cu(In,Ga)Se_2$ devices with efficiency as high as 15.4% by NREL group [17]. However, a physical vapor deposition (PVD) step was required to add In and Ga to readjust the film composition for the processing of photovoltaic devices.

In this work, CIS precursors were synthesized by electrodeposition, then the precursors were annealed in Se vapor using solid Se source to avoid highly toxic H_2Se gas and did not add In element in post annealing treatments. Solar cells with annealed CIS films as absorber were fabricated. The configuration of the solar cells was Al doped ZnO (AZO)/intrinsic ZnO (i-ZnO)/CdS/CIS/Mo/glass as described in Ref.[13]. The crystal structure, morphology, composition, optical and electrical properties of the CIS films were investigated. The CIS solar cell performances were tested using current *vs.* voltage (I-V) measurements in dark condition and illuminated conditions.

II. EXPERIMENTS

The CIS precursors were electrodeposited on 3 cm×3 cm square Mo (thickness of 800 nm) coated soda-lime glass substrates. Three electrode systems with aquatic solutions containing analytical reagents $CuSO_4$, $In_2(SO_4)_3$, H_2SeO_3, and Na_2SO_4 were used. The concentration of solution was chosen to be 3 mmol/L $CuSO_4$, 3 mmol/L $In_2(SO_4)_3$, 5 mmol/L H_2SeO_3, and 0.1 mol/L Na_2SO_4 which was chosen to be supporting electrolyte. The solution pH value was adjusted to be 2.2 by the addition of H_2SO_4. Electrodeposition was carried out in a potentiostatic mode at −0.55 V *vs.* saturated calomel electrode (SCE) us-

*Author to whom correspondence should be addressed. E-mail: cfzhu@ustc.edu.cn, Tel.: +86-551-3600578, FAX: +86-551-3601958

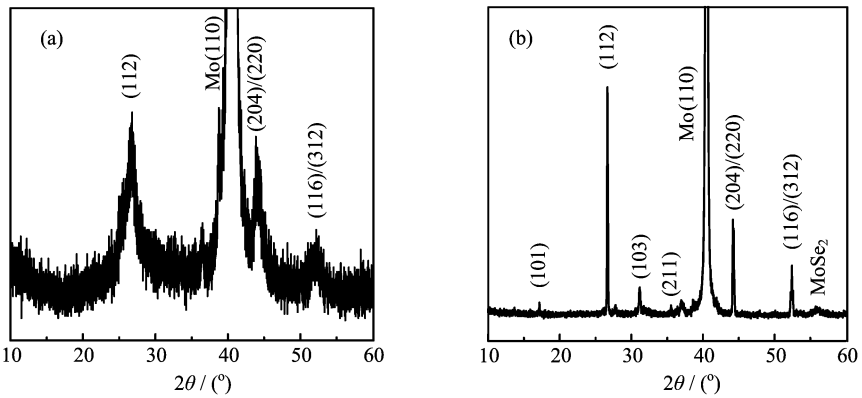

FIG. 1 XRD patterns of (a) as-electrodeposited CIS film and (b) the film annealed in Se vapor at 530 °C for 20 min.

ing an electrodeposition station (CHI 660C). The thickness of the films was controlled by coulometric measurements. Then the samples were cut into 1 cm×1 cm square pieces for annealing.

Annealing of the as-deposited films in the atmosphere of Se vapor was carried out in a two-zone furnace. The detailed annealing procedure was described elsewhere [18]. The temperature of samples was kept at 530 °C and the temperature of Se source was kept at 380 °C, the heating rate was 60 K/min, the annealing time was 20 min. At the end of annealing, the samples were cooled at a rate of 5 K/min to avoid the film peeling off from the substrates. The morphology and compositions of the CIS films were examined by a field emission scanning electron microscope (FE-SEM, FEI Sirion 200) and an energy dispersive X-ray (EDX) spectroscope. The crystalline structures were characterized by powder X-ray diffraction (XRD, MXPAHF diffractometer with Cu Kα radiation, λ=1.5406 Å). Raman measurements were performed at room temperature using a LABRAM-HR micro-Raman system in the back scatting configuration with a laser source of 514 nm and a light-beam diameter of 20 μm. Optical characterizations of the CIS films have been carried out at room temperature using a UV/VIS/NIR spectrophotometer (SHIMADZU DUV-3700).

The electrical properties of the annealed CIS films were tested by measuring the admittance spectra of Al/CIS Schottky junctions. Before preparing the Schottky junctions and fabricating the solar cells, KCN etching was carried out to remove the $Cu_{2-x}Se$ compounds from the annealed film surface as described in Refs.[19, 20]. Some Al circle spots (2 mm diameter) were evaporated on the etched CIS films using thermal evaporation using 99.999% purity Al wires as targets, and the thickness of Al films was about 2 μm. The admittance spectra of Schottky junctions were tested using an electrochemical station (IM6ex, Zahner). The measurements were carried out at the frequencies in the range from 10 Hz to 1 MHz with the magnitude of incremental voltage set at 20 mV. Photovoltaic devices (PV) were fabricated by the sequential deposition of CdS, highly resistant i-ZnO, and highly conductive AZO layers on the treated CIS layer. The CdS was deposited using chemical bath deposition (CBD) method similar to that described by Contreras *et al.* [21]. The i-ZnO and AZO layer were deposited by pulse laser deposition (PLD). A KrF laser (wavelength: 248 nm, 5 Hz) was used to ablate an undoped ZnO target and an Al_2O_3 doped (2%) ZnO target for i-ZnO and AZO layer deposition, respectively. The substrate was maintained at a temperature of 200 °C during the PLD process.

The performance of the solar cells was evaluated under standard AM 1.5 conditions (1 kW/m^2, 25 °C) using an Oriel Sol3A solar simulator, and the *I-V* measurements were carried out using a Keithley 2400 sourcemeter.

III. RESULTS AND DISCUSSION

Figure 1 show the XRD results for the as-deposited and annealed CIS films in Se vapor. These results indicate that both the samples have the chalcopyrite structure (tetragonal JCPDS 89-5649, a=5.790 Å, c=11.618 Å) as the major CIS phase. The as-deposited CIS film displays three broad main diffraction peaks corresponding to (112), (204)/(220), and (116)/(312) planes as shown in Fig.1(a), indicating poor crystallinity. In general, the grain size D can be calculated by the Scherrer formula using (112) peak:

$$D = \frac{0.89\lambda}{\beta \cos\theta} \tag{1}$$

where β refers to the full width at half maximum (FWHM), θ refers to Bragg angle, and λ equals 0.154056 nm. The grain size is estimated to be about 5 nm.

Recently, we studied the annealing at high temperature with a fast heating rate can improve the grain size of CIS films and reduce the formation of Cu-Se compounds [18]. After annealing at 530 °C for 20 min in Se

DOI:10.1088/1674-0068/24/02/225-230

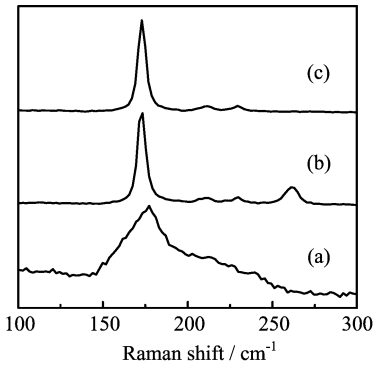

FIG. 2 Raman spectra of (a) as-electrodeposited CIS film, (b) annealed film in Se vapor, and (c) annealed film followed by KCN-treating.

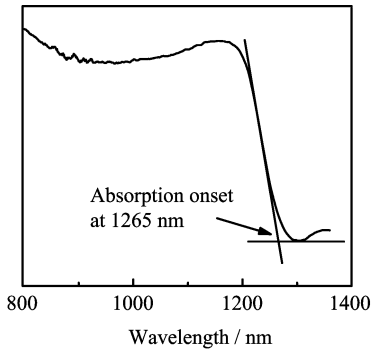

FIG. 3 Room temperature absorbance spectrum of annealed CIS film on Mo coated glass substrate.

TABLE I The compositions of the CIS films determined by EDX method.

	Cu/%	In/%	Se/%	Cu/In	Se/(Cu+In)
As-deposited	25.1	28.0	46.9	0.90	0.88
Annealed	23.7	27.8	48.5	0.85	0.94
KCN treated	22.9	30.8	46.2	0.75	0.86

vapor, the materials crystallinity was improved as the XRD peaks are sharper and more distinguished after annealing (Fig.1(b)). All peaks observed on the patterns were well in accord with the diffraction lines in the chalcopyrite structure of CIS. However, a conductive Cu-Se second phase is usually known to be formed on the surfaces and grain boundaries after annealing process, and it causes a short circuit during device fabrication [22, 23]. It is known that dipping in KCN solution can effectively remove Cu-Se compounds from CIS surface [19, 20]. Before preparing the solar cells, chemical etching was carried out to remove the Cu-Se compounds from the annealed film surface to improve the electrical properties of CIS films. Figure 2 depicts the Raman spectra of the as-electrodeposited CIS film, the film annealed at Se vapor and the film annealed followed by KCN etching, respectively. All spectra are normalized to the most intensive peak. A broad peak centered at 177 cm^{-1} is observed in Fig.2(a). The peak centered at 177 cm^{-1} shows a significant blue shift in relation to the frequency of the chalcopyrite CIS A_1 mode (173 cm^{-1}) [24]. This shift could be related to the presence of a high density of defects in the scattering volume or to a nanocrystalline structure or to residual stress [25, 26]. The elementary selenium is identified by the peak at 240 cm^{-1} which is due to trigonal selenium [27]. These results suggest the as-electrodeposited films were nanocrystalline and accompanied by other phases such as element Se and Cu-Se compounds. Figure 2(b) shows the chalcopyrite A_1 mode at 173 cm^{-1}, $B_2(E)$ mode at 212 and 229 cm^{-1} [28]. The peak at 260 cm^{-1} corresponds to the Cu-Se binary compounds [19, 29]. After KCN treatments the peak at 260 cm^{-1} disappeared while other peaks remain relatively unchanged as shown in Fig.2(c), indicating successfully removing the Cu-Se compounds from the annealed CIS films.

The compositions of the CIS films were determined by EDX measurements. As displayed in Table I, the atom ratio of Cu/In/Se is close to 1/1/2 for the as-electrodeposited CIS films. It can be found that the ratio of Cu/In/Se changed slightly after annealing and etching. The Se component increased after annealing at Se vapor, and the Cu and Se component decreased after KCN treatment due to some Cu-Se compounds were dissolved.

Since the CIS films were synthesized on light-tight substrates, the optical absorbance of the electrodeposited-annealed CIS films were estimated by measuring diffuse reflectance spectrum as a function of wavelength [15, 30], and the results are shown in Fig.3. Measurements were made in the wavelength range from 800 nm to 1400 nm. There is an abrupt increase in the absorption spectrum. The absorption edge is at 1265 nm and the band gap of the CIS film is evaluated to be 0.98 eV, which is consistent with their bulk band gap energies of 0.95−1.04 eV [31].

Figure 4(a) illustrates the cross-sectional SEM image of the as-electrodeposited CIS film. The CIS film with thickness about 1 μm is compact, uniform, and adherent. The crystallinity was improved after annealing in Se vapor as shown in Fig.4(b), and there are some platelets on the surface of CIS film which are attributed to Cu-Se binary compounds. However, the platelets were not observed after dipping samples into KCN solution as shown in Fig.4(c), indicating that the Cu-Se compounds were removed, which is coherent with the Raman results. Figure 4(d) depicts the cross section of a fabricated solar cell using the treated CIS film as an absorber. The formation of $MoSe_2$ interlayer was observed as a result of diffusion of Se through CIS and following reaction with Mo back contact. The $MoSe_2$ layer was beneficial for the cell performance because of forming ohmic back contact, improving adhesion of the absorber to Mo back contact and reducing the recombination at the back contact [16]. It is observed that

DOI:10.1088/1674-0068/24/02/225-230

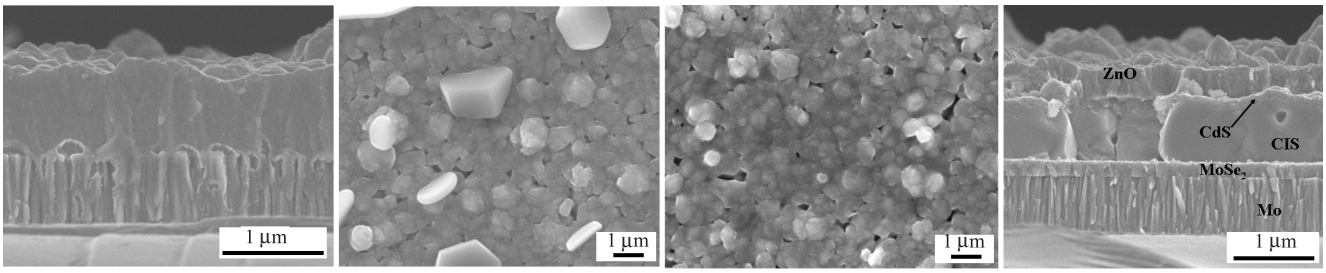

FIG. 4 SEM images of (a) cross section of as-deposited CIS film, (b) plane view of the annealed CIS film, (c) plane view of the annealed film followed by KCN-treating, and (d) cross section of a fabricated solar cell using the CIS film as the absorber.

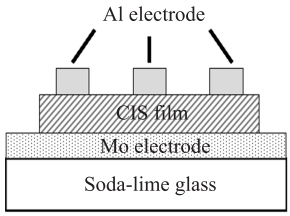

FIG. 5 Schematics of the Al/CIS Schottky junctions.

the annealed CIS film consists of relatively large grains in the range of 500−1000 nm and single grain of films extend usually through the whole film thickness. This film is suited to fabricate the photovoltaic devices. The thickness of CdS layer and ZnO layer are about 100 and 450 nm as displayed in Fig.4(d).

Figure 5 show the schematics of the Al/CIS junctions. Figure 6 (a) show the I-V characteristic curve of the Al/CIS junctions. The rectifying behavior confirms that the Al/CIS junctions behave as well-defined pn diodes, and the conductive type of CIS films is p type. The C-V characteristic curves of the Al/CIS diode at room temperature were measured at frequencies of 5, 10, 30, and 50 kHz, which were plotted in the form of C^{-2}-V, as shown in Fig.6(b). The plots show linear behavior, suggesting that the diode is an abrupt junction. According to the theory of Schottky junction, the carrier concentrations of CIS films can be derived from Eq.(2):

$$N_A = \frac{2}{A^2 q \varepsilon_s} \left(\frac{\mathrm{d}C^{-2}}{\mathrm{d}V} \right)^{-1} \tag{2}$$

where N_A is the effective carrier concentration in CIS films, A is the area of Schottky junction, q is the charge of an electron, ε_s is the relative permittivity of CIS (ε_s=13.6 [32]). The carrier concentrations derived at 5, 10, 30, and 50 kHz are 4.65×10^{16}, 4.91×10^{16}, 5.03×10^{16}, and 4.38×10^{16} cm^{-3}, respectively.

It is noted that the slope of C^{-2}-V curves varies with the frequency but with a very small change, and the effective carrier concentration in the thin film Schottky

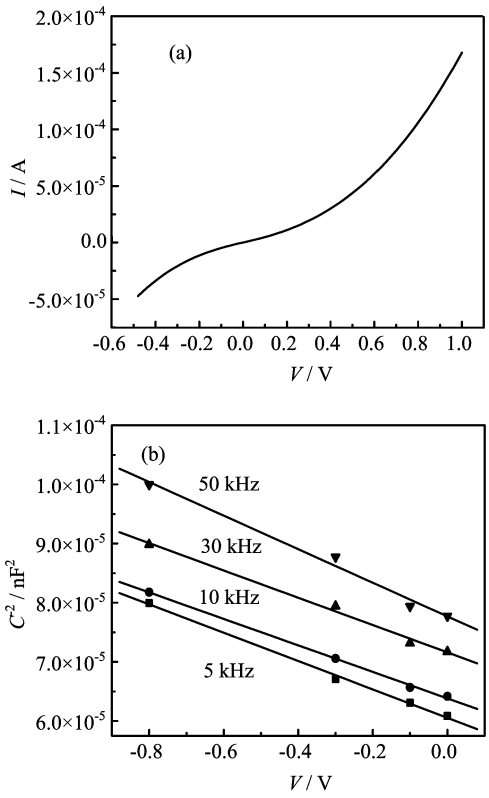

FIG. 6 (a) I-V curve of the Al/CIS Schottky junction and (b) C^{-2}-V curves of the Al/CIS Schottky junction at different frequencies.

junctions is in the order of 10^{16} cm^{-3}. This concentration is favorable for preparing of solar cells. Combined with the EDX results in Table I, the KCN treated CIS films are Cu deficient, Se deficient and In rich. The CIS films are strong self-compensation, and the composition ratio needs to be further optimized.

The performance of the fabricated solar cell with an area of 0.2 cm^2 was analyzed by measuring the current density *vs.* voltage (J-V) curves characteristics under dark and light illumination conditions. Figure 7 illustrate the J-V curves corresponding to dark and

DOI:10.1088/1674-0068/24/02/225-230

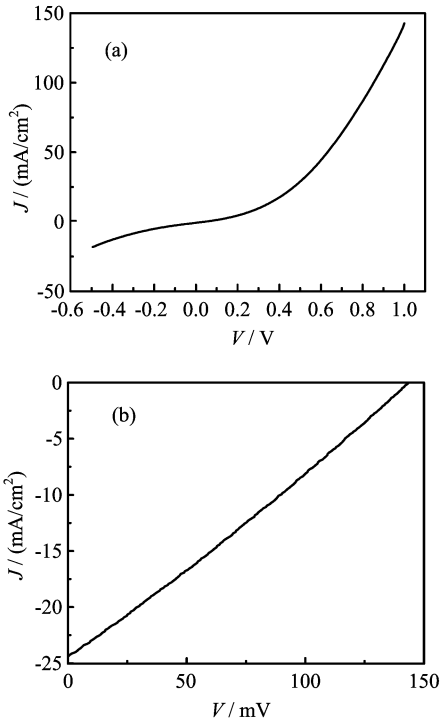

FIG. 7 J-V curves of the solar cells (a) under dark, and (b) under light conditions (AM 1.5, 100 mW/cm^2, 25 °C). V_{oc}=144 mV, J_{sc}=24.4 mA/cm^{-2}, FF=27.2%, η=0.96%.

light conditions. The cell parameters were found to be V_{oc}=144 mV, J_{sc}=24.4 mA/cm^2, fill factor FF=27.2%, and conversion efficiency η=0.96%, respectively. The low V_{oc} is attributed to the large recombination loss behaving as large reverse leakage current as shown in Fig.7(a). It may be caused by large defect density at the interface of the junction or some pin holes in the films which leaded to a current leakage path. The small FF indicates that there are low shunt resistance and voltage-dependent current collection in solar cells. According to the basic principles of solar cells [33], the V_{oc} and I_{sc} have the following relation:

$$V_{oc} = \frac{kT}{q} \ln\left(\frac{J_{sc}}{J_0}\right) \tag{3}$$

where q is the charge of an electron, J_0 is the reverse saturation current density in dark conditions.

From Fig.7(a) it can be seen that J_0 is in the miliampere order of magnitude, which is much higher than the reverse saturation current density of the high efficiency solar cells [34], thus the V_{oc} is lower in our experiments. Further fine measurements need to be carried out to distinguish the detailed effect parameters. The limited efficiency was perhaps caused by the high interface defect density, small shunt resistance. To obtain a better efficiency, optimizing the device fabricating process and improving the interface quality are needed in the future work.

IV. CONCLUSION

The CIS thin films with good crystallinity have been obtained by selenizing the electrodeposited Cu/In/Se precursors at 530 °C in low toxic Se atmosphere. The XRD and Raman spectra suggested that the annealed CIS films had a chalcopyrite structure. The bandgap of the annealed CIS films was estimated to be 0.98 eV from absorption spectroscopy. C-V tests of Al/CIS Schottky junctions revealed that the carrier concentration of annealed CIS films was in the order of 10^{16} cm^{-3} after etching the Cu/Se binary compounds by KCN solution. Solar cells with the treated CIS films as absorbers and with the structure of AZO/i-ZnO/CdS/CIS/Mo/glass were fabricated. The device with an area of 0.2 cm^2 had V_{oc}=144 mV, J_{sc}=24.4 mA/cm^{-2}, FF=27.2%, and η=0.96% under global AM 1.5 condition. Further improvements of the device fabricating processes would significantly aid the realization of low-cost thin film CIS PV manufacturing.

V. ACKNOWLEDGMENTS

The authors are grateful to J. L. Huang and W. Q. Liu from the Structure Research Laboratory of CAS in Hefei for their assistances of the measurements of SEM and UV-VIS-NIR spectroscopy with this work. This work was supported by the Knowledge Innovation Project of the CAS (No.KJCX2-YW-M11), and the CAS Special Grant for Postgraduate Research, Innovation and Practice.

[1] I. Repins, M. A. Contreras, B. Egaas, C. DeHart, J. Scharf, C. L. Perkins, B. To, and R. Noufi, Prog. Photovolt. Res. Appl. **16**, 235 (2008).
[2] P. J. Dale, A. P. Samantilleke, G. Zoppi, I. Forbes, and L. M. Peter, J. Phys. D **41**, 085105 (2008).
[3] S. Ishizuka, H. Shibata, A. Yamada, P. Fons, K. Sakurai, K. Matsubara, and S. Niki, Appl. Phys. Lett. **91**, 041902 (2007).
[4] H. Zachmann, S. Heinker, A. Braun, A. V. Mudryi, V. F. Gremenok, A. V. Ivaniukovich, and M. V. Yakushev, Thin Solid Films **517**, 2209 (2009).
[5] J. X. Yang, Z. G. Jin, Y. T. Chai, H. Y. Du, T. J. Liu, and T. Wang, Thin Solid Films **517**, 6617 (2009).
[6] R. Wuerz, A. Eicke, M. Frankenfeld, F. Kessler, M. Powalla, P. Rogin, and O. Yazdani-Assl, Thin Solid Films **517**, 2415 (2009).
[7] L. Oliveira, T. Todorov, E. Chassaing, D. LinCot, J. Carda, and P. Escribano, Thin Solid Films **517**, 2272 (2009).
[8] F. D. Jiang and J. Y. Feng, Thin Solid Films **515**, 1950 (2006).
[9] M. Wang, Z. W. Zhang, G. S. Jiang, and C. F. Zhu, Chin. J. Chem. Phys. **23**, 363 (2010).
[10] S. Taunier, J. Sicx-Kurdi, P. P. Grand, A. Chomont, O. Ramdani, L. Parissi, P. Panheleux, N. Naghavi, C.

DOI:10.1088/1674-0068/24/02/225-230

Hubert, M. Ben-Farah, J. P. Fauvarque, J. Connolly, O. Roussel, P. Mogensen, E. Mahe, J. F. Guillemoles, D. Lincot, and O. Kerrec, Thin Solid Films **480**, 526 (2005).
[11] J. F. Guillemoles, P. Cowache, A. Lusson, K. Fezzaa, F. Boisivon, J. Vedel, and D. Lincot, J. Appl. Phys. **79**, 7293 (1996).
[12] V. Izquierdo-Roca, X. Fontane, J. Alvarez-Garcia, L. Calvo-Barrio, A. Perez-Rodriguez, J. R. Morante, C. M. Ruiz, E. Saucedo, and V. Bermudez, Appl. Phys. Lett. **94**, 061915 (2009).
[13] C. Sene, M. E. Calixto, K. D. Dobson, and R. W. Birkmire, Thin Solid Films **516**, 2188 (2008).
[14] D. L. Xia, M. Xu, J. Z. Li, and X. J. Zhao, J. Mater. Sci. **41**, 1875 (2006).
[15] S. H. Kang, Y. K. Kim, D. S. Choi, and Y. E. Sung, Electrochim. Acta **51**, 4433 (2006).
[16] M. Kemell, M. Ritala, and M. Leskela, Crit. Rev. Solid State Mater. Sci. **30**, 1 (2005).
[17] R. N. Bhattacharya, J. F. Hiltner, W. Batchelor, M. A. Contreras, R. N. Noufi, and J. R. Sites, Thin Solid Films **361**, 396 (2000).
[18] Z. W. Zhang, J. Li, M. Wang, M. Wei, G. S. Jiang, and C. F. Zhu, Solid State Commun. **150**, 2346 (2010).
[19] W. Li, Y. Sun, W. Liu, F. Y. Li, and L. Zhou, Chin. Phys. **15**, 878 (2006).
[20] M. Kemell, M. Ritala, and M. Leskela, J. Mater. Chem. **11**, 668 (2001).
[21] M. A. Contreras, M. J. Romero, B. T. F. Hasoon, R. Noufi, S. Ward, and K. Ramanathan, Thin Solid Films **403**, 204 (2002).
[22] S. Niki, P. J. Fons, A. Yamada, Y. Lacroix, H. Shibata, H. Oyanagi, M. Nishitani, T. Negami, and T. Wada, Appl. Phys. Lett. **74**, 1630 (1999).
[23] T. Wada, N. Kohara, T. Negami, and M. Nishitani, J. Mater. Res. **12**, 1456 (1997).
[24] C. Rincon and F. J. Ramirez, J. Appl. Phys. **72**, 4321 (1992).
[25] V. Izquierdo-Roca, J. Alvarez-Garcia, L. Calvo-Barrio, A. Perez-Rodriguez, J. R. Morante, V. Bermudez, O. Ramdani, P. P. Grand, and O. Kerrec, Surf. Interface Anal. **40**, 798 (2008).
[26] O. Ramdani, J. F. Guillemoles, D. Lincot, P. P. Grand, E. Chassaing, O. Kerrec, and E. Rzepka, Thin Solid Films **515**, 5909 (2007).
[27] V. Izquierdo-Roca, X. Fontane, J. Alvarez-Garcia, L. Calvo-Barrio, A. Perez-Rodriguez, J. R. Morante, J. S. Jaime-Ferrer, E. Saucedo, P. P. Grand, and V. Bermudez, Thin Solid Films **517**, 2163 (2009).
[28] D. Wang, L. Wan, Z. Bai, and Y. Cao, Appl. Phys. Lett. **92**, 211912 (2008).
[29] W. Witte, R. Kniese, and M. Powalla, Thin Solid Films **517**, 867 (2009).
[30] L. Djellal, S. Omeiri, A. Bouguelia, and M. Trari, J. Alloys Compd. **476**, 584 (2009).
[31] S. Beyhan, S. Suzer, and F. Kadirgan, Sol. Energy Mater. Sol. Cells **91**, 1922 (2007).
[32] A. Rockett and R. W. Birkmire, J. Appl. Phys. **70**, R81 (1991).
[33] *Antonio Luque and Steven Hegedus, Handbook of Photovoltaic Science and Engineering*, Chichester: John Wiley & Sons, Ltd., (2003).
[34] M. A. Contreras, K. Ramanathan, J. AbuShama, F. Hasoon, D. L. Young, B. Egaas, and R. Noufi, Prog. Photovolt. Res. Appl. **13**, 209 (2005).

DOI:10.1088/1674-0068/24/02/225-230